RSC Advances

PAPER

View Article Online
View Journal | View Issue

Cite this: *RSC Adv.*, 2024, **14**, 25669

Development and evaluation of antimicrobial PVC-grafted polymer for enhanced paint applications

Sonali Gupta,[a] Yashoda Malgar Puttaiahgowda *[a] and Ananda Kulal[b]

Demand for antimicrobial paints is increasing globally due to the rising need to control microbial growth and reduce infection risks in various environments. This increased demand underscores the crucial role of advanced antimicrobial coatings in promoting health and safety. In this context, an innovative poly(vinyl chloride) (PVC) grafted polymer with 1-(2-aminoethyl piperazine) (AEP) was prepared and studied in detail. In this study, the prepared polymer was characterized using FTIR and NMR spectroscopy to examine the polymer's chemical structure and employed TGA and DSC for thermal stability analysis. The antimicrobial activity of the grafted polymer was evaluated through the agar diffusion method and showed a significant inhibition zone of 21.6 mm for *S. aureus*, 16.3 mm for *E. coli*, 18.3 mm for *M. smegmatis*, and 20.3 mm for *C. albicans* at a lowest concentration of 12.5 μg mL^{-1}. To assess surface characteristics, the PVC-*g*-AEP polymer was mixed with commercial paint and applied to a glass surface. SEM and AFM analysis showed a 5-times increase in porosity while maintaining visual aesthetics. Additionally, the paint displayed excellent stability against water, retaining around 90% of its antimicrobial activity even after 15 washes. This advanced polymer not only exhibits superior antimicrobial properties but also improves paint durability, setting a new benchmark for high-performance antimicrobial coatings and significantly advancing protective paint technology.

Received 7th June 2024
Accepted 5th August 2024

DOI: 10.1039/d4ra04173a

rsc.li/rsc-advances

1. Introduction

A major issue for public health is microbial illnesses; many ecosystems are home to bacteria, fungi, and algae.[1–3] Additional complexity is introduced by biofilm growth on surfaces, which calls for efficient methods of control and prevention.[4] Concerns about surface microbiome contamination have prompted intensive studies on antimicrobial coatings (AMCs).[5–7] An encouraging new approach to dealing with biofilm-related issues is the creation of AMCs, which attempt to inhibit the growth and proliferation of harmful bacteria. The focus is on surface modification using bioactive compounds. These agents work by interacting with the microbiome to restrict growth. Designing surfaces that are impermeable to microbes highlights the significance of logical methods in creating efficient antibacterial solutions.[8–11]

Surface biofilm growth is a major contributor to the problem, so there needs to be a way to effectively avoid and regulate it. Considering the wide variety of technologies available, antimicrobial coatings (AMCs) have thus become an important focus of research. Examples of AMC include antibiotic nanoparticles, chitosan or quaternary ammonium polymers immobilized for contact activation, and light-activated molecules such as TiO_2.[12–14] The main goals of designing antimicrobial surfaces are to release antibacterial agents, kill bacteria upon contact, and prevent adherence. A great way to modify surfaces to create effective anti-adhesive surfaces is with polymers, thanks to their malleable characteristics.[15] All kinds of industries make use of AMCs, from the textile[16,17] and paint industries[18] to healthcare facilities,[19] water purification systems, and food packaging.[20] The use of antimicrobial paints has recently become an important strategy for dealing with biofilm issues in a variety of settings, including homes, businesses, and public areas.[21]

Paint, in a general sense, is a fluid substance that solidifies into a cohesive and adherent film upon thin application to a surface. This category includes enamels, varnishes, undercoats, lacquers, and undercoats, among others. In general, paint formulations comprise a binder or matrix, pigments or dyes to impart color, extenders to impart additional properties, and a solvent,[22] which may be water-based or organic (solvent-based).[23,24] Approximately 5% of the overall system consists of supplementary elements, such as cellulose or polymers, zeolites, bentonites, biocides, defoamers, and additives including thickeners, surfactants, and plasticizers. An evident change is noted in the substitution of solvent-based paints with water-based (latex) paints, which are renowned for their ability to fill binders.[25] An additional method of classifying paints is according to the binder they contain, which can be organic or

[a]*Department of Chemistry, Manipal Institute of Technology, Manipal Academy of Higher Education, Manipal, 576104, Karnataka, India. E-mail: yashoda.mp@manipal.edu*

[b]*Biological Sciences Division, Poornaprajna Institute of Scientific Research, Devanahalli, Bengaluru, 562164, Karnataka, India*

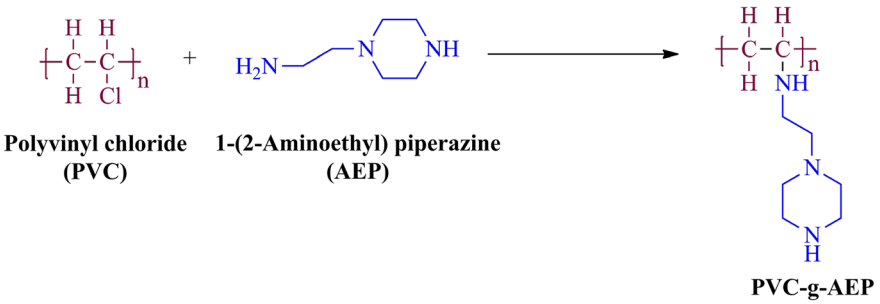

Scheme 1 Schematic representation to obtain PVC-*g*-AEP polymer.

inorganic (*e.g.*, natural latexes or synthetic polymers such as alkyd and acrylic) or sol silicate or silicate paints. Antimicrobial agents, including quaternary ammonium salts, *N*-halamine materials, and acrylics, have been the subject of extensive research and application in the domain of commercial paint preparation.[26–28]

Many studies on the development of antimicrobial paint have been published. Silicon-based polyurethane films with strong antibacterial properties against *Escherichia coli* were created by Sauvet *et al.*, in 1995. They created quaternary ammonium salts (QAS) and hydroxyl groups and synthesized functional polysiloxanes and show promising antibacterial activity against *E. coli* and may find use in paints, binders, elastomers, and mastic compound additives.[29] To create contact-active antimicrobial surfaces, Fuchs *et al.*, (2006) used water-insoluble antimicrobial emulsifiers. The emulsifiers were produced by styrene and 4-vinylpyridine anionic copolymerization, which yielded a block copolymer (PS-*b*-P4VP). These contact-active antimicrobial coatings work on a variety of substrates, including plastics and metals, and can be used as an alternative to biocide-releasing coatings. In commercial paints, the synthesized emulsifiers exhibit encouraging promise as a secure substitute for water-soluble biocides.[30] Mukherjee and colleagues created hydrophobic polycationic coatings designed to kill airborne *E. coli* and *S. aureus* from coughing and sneezing in 2008. The hydrophobic polycation *N*-dodecyl, *N*-methyl-polyethylenimine was coated on glass, wool, nylon, and polypropylene. Coated surfaces were highly effective against *S. aureus* and *E. coli*. Polycation concentration and organic solvent type affected bactericidal efficiency. Glass slides coated with 50 mg mL^{-1} polymeric solution were 100% bactericidal. The painted fabric lost bactericidal action slightly after repeated laundry cycles. However, the painted surfaces were poisonous to mammalian cells, presenting concerns for different applications.[31] Haldar *et al.*,[32] (2014) developed organo-soluble and water-insoluble polymer pigments from polyethylenimine (PEI) through the Eschweiler–Clarke reaction and quaternization with bromoalkanes. A variety of polymers were synthesized, comprising branched PEIs and linear PEIs. The polymers demonstrated effective antibacterial and antifungal properties when tested against a range of pathogens, such as *Cryptococcus* spp., *Pseudomonas aeruginosa*, methicillin-resistant *Staphylococcus aureus* (MRSA), and *Klebsiella pneumoniae*. The hydrophobic polymers that were synthesized demonstrated potential as antimicrobial paints for commercial and biomedical purposes. When applied to glass transparencies along with commercial paint and medical-grade polymer polylactic acid (PLA), these polymers exhibited 100% activity against *E. coli* and *S. aureus*.[32] In the present study, we successfully synthesized PVC-*g*-AEP using graft polymerization techniques and subsequently incorporated this polymer into commercially available paint formulations. The primary objective was to evaluate the antimicrobial effectiveness of the modified paint, providing insights into its potential for enhancing surface protection against microbial growth.[32]

2. Experimental

2.1. Materials and methods

1-(2-Aminoethyl)piperazine (AEP) was purchased from Carbanio company with 99% purity. Piperazine (PZ), triethylamine (TEA), and polyvinyl chloride (PVC; average molecular weight) were purchased from Sigma-Aldrich with <99% purity. Tetrahydrofuran (THF) and water were used as solvents for synthesis and extraction and used as received. The paintbox was purchased from a local market in Eshwar Nagar, Manipal, Udupi District, Karnataka, India.

2.2. Synthesis of PVC-*g*-AEP polymer

To synthesize PVC grafted AEP polymer, 0.01 mol (0.625 g) of commercially available PVC was dissolved in THF solvent and 0.01 mol (1.3 mL) of AEP was added to the reaction mixture. The TEA was added to create a basic environment in the mixture and the reaction was stirred for 24 h at 80 °C. The PVC-*g*-AEP (Scheme 1) was obtained upon extraction with water and a white color product was formed which was washed with THF solvent several times to remove unreacted reactants.

3. Characterizations

3.1. Structural characterization

The FTIR spectrum of PVC-*g*-AEP polymer was recorded using Shimadzu-8400S FTIR spectrophotometer in the range of 400–4000 cm^{-1}. The ^1H NMR spectrum was recorded using a Bruker spectrometer using TMS as an internal reference and solvent-deuterated DMSO. Using a TA Instruments SDT-Q600, the

thermal properties of PVC-*g*-AEP polymer were investigated. Thermogravimetric analysis (TGA) and differential scanning calorimetry (DSC) thermograms of the synthesized polymer were acquired using aluminium trays heated at a rate of 10 °C min^{-1} in a nitrogen atmosphere over a temperature range of 25–800 °C. Scanning electron microscopy (SEM) is utilized to observe the polymer that has been deposited on glass. A working voltage of 20 kV was used to take scanning electron microscopy images using a ZEISS EVO MA18 with a variety of pressure modes. Atomic force microscopy (AFM) is used to image the topography of materials in their native environments. AFM images were obtained using Bruker Innova IB342.

3.2. Antimicrobial activity

The antimicrobial activity of the PVC–AEP polymer was evaluated using a diffusion assay method against different microorganisms, including *Staphylococcus aureus* (a Gram-positive bacterium, strain MTCC 3160), *Escherichia coli* (a Gram-negative bacterium, strain MTCC 1687), *Mycobacterium smegmatis* (a variant of tuberculosis, strain MTCC 944), and *Candida albicans* (a fungus, strain MTCC 7253). The experiment utilized bacterial and fungal strains obtained from the microbial type culture collection (MTCC) at the Institute of Microbial Technology in Chandigarh. These strains were acquired by the Poornaprajna Institute of Scientific Research in Bengaluru, Karnataka. The antimicrobial activity was conducted following the procedure outlined by the Clinical and Laboratory Standards Institute (CLSI). The zone of inhibition (ZoI) was measured using a standardized scale.

To assess the antimicrobial properties of the polymer, 100 μL of bacterial cultures (*S. aureus*, *E. coli*, and *M. smegmatis*) and fungal culture (*C. albicans*) were added to nutritional broth media. The mixtures were then incubated in a shaker incubator at 37 °C for 12 hours at a speed of 120 rpm. The commercially available nutrient agar media was prepared and sterilized using an autoclave. Approximately 30 mL of the molten medium was then poured into Petri plates inside the laminar airflow (LAF) system aseptically. The plates were left undisturbed for approximately 30 min to allow the medium to solidify. Subsequently, the 12 h old bacterial and fungal cultures were retrieved from the shaker incubator and diluted in a series according to the 0.5 McFarland (10^{-4} times dilution) standard and spread onto nutrient agar media using a sterile cotton earbuds. The sample solution was prepared by dissolving a 10 mg polymer sample in 1 mL of THF and 100 μL was taken from the prepared polymer solution followed by serial dilution to obtain four different concentrations: 100, 50, 25, and 12.5 μg mL^{-1}. Then 5 μL of each sample was transferred on a Petriplate containing microbial lawn at four different places and incubated overnight at 37 °C. Similarly, cephalothin discs (30 μg per disc) were used as an antibacterial standard on all three bacterial plates (*S. aureus*, *E. coli*, and *M. smegmatis*), while 5 μL of fluconazole (10 mg mL^{-1}) was used as an antifungal standard for *C. albicans*. The THF solvent was also tested for its antimicrobial activity as a negative control. The zone of inhibition by each concentration of samples was measured using a scale and tabulated.

3.3. Antimicrobial activity of painted glass slides

Using the method outlined above, the bacterial plates were prepared. Three sets of glass slides were prepared; set 1: painted glass slide without polymer; set 2: painted glass slide with polymer and set 3: painted glass slide with polymer and washed with water for 15 cycles, all these are tested for their antimicrobial activity against *C. albicans* (fungi), *E. coli* (Gram-negative bacteria), and *S. aureus* (Gram-positive bacteria). The efficacy of the painted slide with polymer was also determined, for that, the painted slide with polymer was washed 15 times in Milli-Q water and afterward tested for antimicrobial activity. To perform the activity, three different glass slides (one from each set) were placed on the microbial lawn in different microorganisms and checked for their antimicrobial activity.

4. Results and discussion

The reaction between polyvinyl chloride (PVC) and aminoethyl piperazine (AEP) involves grafting AEP onto the PVC backbone. Initially, PVC, which is normally inert, is activated through dehydrochlorination to create reactive sites. These sites then react with the amine groups of AEP, forming covalent bonds and effectively grafting the AEP onto the PVC chain. This modification imparts antimicrobial properties to the PVC, making it suitable for applications where microbial resistance is essential. Implementing piperazine-based polymers for antimicrobial paint applications on a large scale requires careful consideration of both costs and processes. The synthesized polymer was characterized for its structural confirmation using FTIR and NMR.

4.1. FTIR analysis

In the FT-IR spectrum of PVC-*g*-AEP, several key bands are evident as represented in Fig. 1. These include the CH_2 asymmetric and symmetric stretching bands at 2972 cm^{-1} and 2883 cm^{-1}, the C–H bending band near Cl at 1215 cm^{-1}, the C–C stretching range between 1000 and 1100 cm^{-1}, and the presence of C–Cl gauche bonds in the region covering from 600

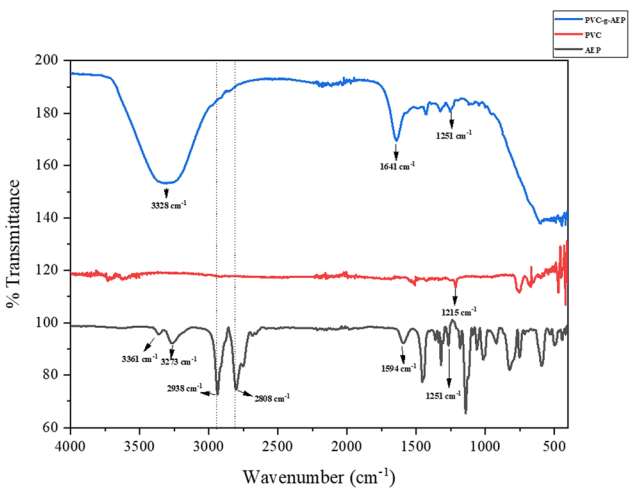

Fig. 1 FTIR spectra of PVC, AEP, and PVC-*g*-AEP polymer.

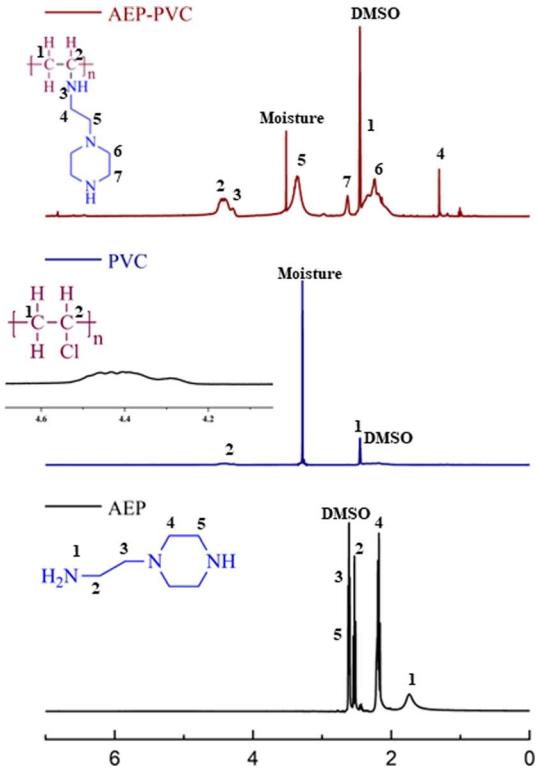

Fig. 2 ^{1}H-NMR spectra of synthesized polymer, PVC, and AEP.

to 650 cm^{-1}. These evident bands offer valuable information regarding the molecular structure and bonding attributes of PVC.[33] The bands at 3273 and 3361 cm^{-1} correspond to amine stretching frequency and the peak corresponding to C–N stretching was observed at 1251 cm^{-1} of AEP. In general, NH in-plane bending vibrations of amines are detected in the range of 1640–1560 cm^{-1}, and it was observed at 1641 cm^{-1} in the PVC-*g*-AEP spectrum. The broad band around 3328 cm^{-1} in AEP-*g*-PVC corresponds to *N*–H stretching vibrations and the C–Cl band disappeared at 1215 cm^{-1} in the polymer spectrum. This implies that the polymer has been formed and further confirmed using ^{1}H-NMR.

4.2. Proton nuclear magnetic resonance spectroscopy (^{1}H-NMR)

The ^{1}H-NMR spectrum of PVC-*g*-AEP is depicted in Fig. 2. The chemical shift observed at $\delta = 2.46$ ppm corresponds to the secondary carbon atom (CH_2^{1}) of the PVC backbone in the polymer which is evident from the PVC spectrum in which the peak was observed at $\delta = 2.5$–2.1 ppm. In addition, the protons corresponding to the tertiary carbon atom (CH^{2}) of PVC were attributed a chemical shift of 4.41 ppm which is similar to 4.6–4.2 ppm as reported elsewhere.[34] The chemical shift found at $\delta = 4.45$ ppm corresponds to the secondary amine (NH^{3}) of AEP in the polymer which converted from primary amine (NH_2^{1}: $\delta = 1.73$ ppm) after polymer formation. The protons of secondary carbon atoms of the AEP backbone in the polymer were attributed at chemical shifts 1.32 (CH_2^{4}) and 3.34 (CH_2^{5}) ppm. The protons of secondary carbon atoms ($CH_2^{6,7}$) of the piperazine ring of AEP were observed at $\delta = 2.33$ and 2.67 ppm which was evident from protons ($CH_2^{4,5}$) observed in AEP molecule ($\delta = 2.17$ and 2.63 ppm). The chemical shift of DMSO solvent corresponds to $\delta = 2.5$ ppm. The NMR observed for the synthesized compounds confirms the formation of the polymer.

4.3. Thermal analysis

The PVC–AEP thermogram is illustrated in Fig. 3. PVC–AEP degraded in two stages at 178.70 and 399.21 °C. The initial phase of weight loss commences at approximately 25 °C, potentially attributable to the existence of water. The respective rates of mass loss transitions are determined to be 8.71%, 47.22%, and 24.17% and calculated as per the eqn (1)–(3) mentioned below. The half-weight loss occurred at a temperature of 242.92 °C, which corresponds to the polymer's half-decomposition temperature ($T_{1/2}$).

$$\text{Rate of mass loss } (\text{mL}_1) = \left[\frac{mA_1 - mB_1}{mA_1}\right] \times 100 \quad (1)$$

$$\text{Rate of mass loss } (\text{mL}_1) = \left[\frac{mA_2 - mB_2}{mA_1}\right] \times 100 \quad (2)$$

$$\text{Rate of mass loss } (\text{mL}_1) = \left[\frac{mA_3 - mB_3}{mA_1}\right] \times 100 \quad (3)$$

Based on the available weight loss data, it can be observed that the beginning of heat treatment is associated with the occurrence of weight loss. Table 1 displays three distinct weight

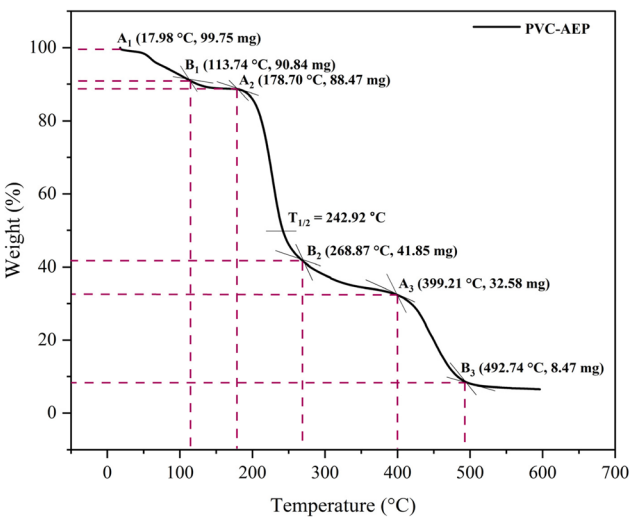

Fig. 3 TGA thermogram of synthesized PVC-*g*-AEP polymer.

Table 1 Thermal properties of PVC-*g*-AEP polymer

Major weight loss transitions (°C)	Rate of mass loss (%)	$T_{1/2}$ (°C)
17.98–113.74	8.71	242.92
178.70–268.87	47.22	
399.21–492.74	24.17	

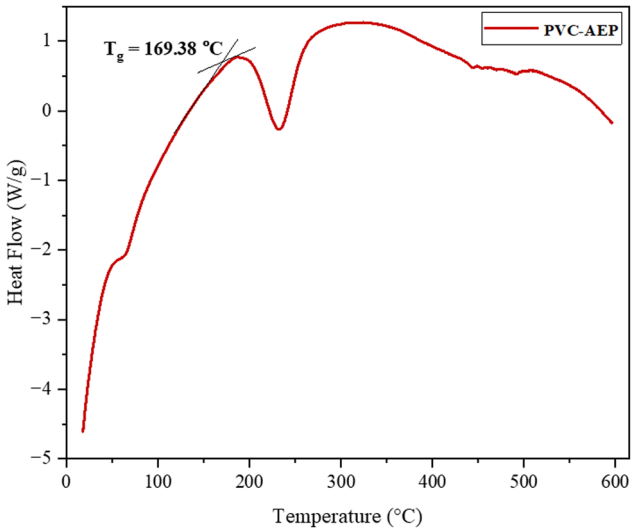

Fig. 4 DSC thermogram of synthesized polymer.

losses occurring within different temperature ranges: 17.98 to 113.74 °C, 178.70 to 268.87 °C, and 399.21 to 492.74 °C. Thermal stability refers to the capacity of a polymeric substance to endure the effects of heat. Based on the thermogravimetric analysis (TGA) thermogram, it has been determined that PVC–AEP has thermal stability up to a temperature of 492.74 °C, beyond which it undergoes decomposition.

The DSC thermogram of PVC–AEP is given in Fig. 4. When examining the temperature-dependent behavior of a polymer, a critical thermal reaction that is of primary importance is the glass transition. This transition leads to a transformation from the state of glass to the rubbery phase. The glass transition temperature (T_g) of PVC–AEP is observed at 169.38 °C.

4.4. Antimicrobial activity

The synthesized grafted polymer demonstrated substantial antimicrobial activity, with significant inhibition zones observed against *S. aureus*, *E. coli*, *M. smegmatis*, and *C. albicans*. The diameter of the zone of inhibition was measured for the different concentrations of PVC-*g*-AEP against three bacteria and one fungus are represented in Fig. 5. The amount of inhibition of microorganisms by 100 μg, 50 μg, 25 μg, and 12.5 μg of PVC-*g*-AEP ranged from 18.6 to 24 mm in the case of *S. aureus*, 16.30 to 19.60 mm for *E. coli*, 16.30 to 18.30 mm for *M. smegmatis* and 17.00 to 23.00 mm for *C. albicans*. There are no significant differences found in the inhibition zone between the low and higher concentrations of PVC-*g*-AEP. The results from the set parameters indicate that even a lower concentration of the polymer can significantly inhibit microbial growth. The inhibition shown by the PVC-*g*-AEP against the microorganisms is comparable to the inhibition zone shown by the standards which is in the range of 27–30 mm as shown in Table 2. The results revealed that the polymer maintained impressive antimicrobial efficacy even at the lower concentrations. PVC-*g*-AEP was particularly effective against *S. aureus*, showing superior activity compared to the other tested microorganisms and values are very near to the standards.

The polymer showed excellent activity against all the tested microbes and the PVC-*g*-AEP demonstrates strong antimicrobial activity mainly due to the inclusion of piperazine. The action

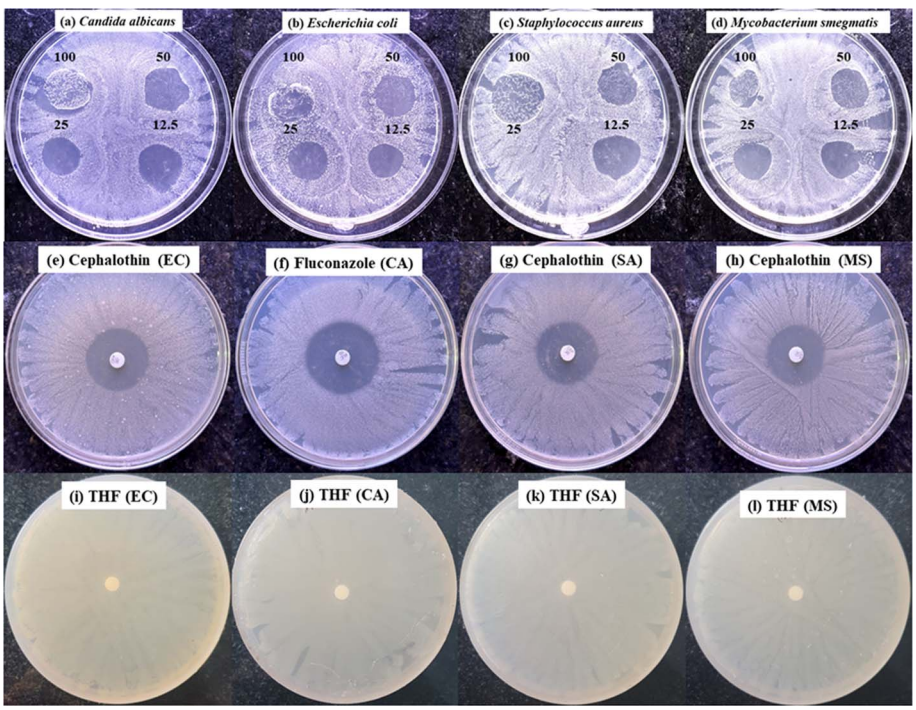

Fig. 5 The inhibition zones exhibited by synthesized polymer: (a) *Candida albicans* (CA), (b) *Escherichia coli* (EC), (c) *Staphylococcus aureus* (SA), and (d) *Mycobacterium smegmatis* (MS). The cephalothin was used as an antibacterial standard for (e) EC, (g) SA, and (h) MS and fluconazole for (f) CA as an antifungal standard. (i–l) Tetrahydrofuran (THF) solvent as control.

Table 2 Antimicrobial assay of PVC-*g*-AEP polymer[a]

Polymer sample concentration (μg mL^{-1})	Zone of inhibition (mm) (mean ± SD, $n = 3$) of different microorganisms			
	S. aureus	*E. coli*	*M. smegmatis*	*C. albicans*
100	24.00 ± 1.0	18.60 ± 2.5	16.30 ± 0.5	23.00 ± 2.0
50	18.60 ± 0.5	19.60 ± 0.5	18.30 ± 0.5	20.60 ± 1.5
25	Error	18.60 ± 1.5	17.60 ± 1.5	17.00 ± 1.0
12.5	21.60 ± 1.5	16.30 ± 0.5	18.30 ± 2.5	20.30 ± 0.5
CP (30 mg)	27.00 ± 0.0	27.60 ± 0.5	26.60 ± 0.5	—
FL (50 mg)	—	—	—	31.60 ± 0.5

[a] CP: cephalothin antibacterial standard, FL: fluconazole is antifungal standard.

mechanism starts with the polymer attaching to the microbial cell surface through electrostatic and hydrophobic interactions. The piperazine groups, which are positively charged, are drawn to the negatively charged microbial cell membranes, disrupting them by increasing their fluidity and permeability. This disruption creates pores, leading to the uncontrolled leakage of intracellular substances such as ions and metabolites. This leakage disturbs the cell's osmotic balance and depletes essential nutrients, impairing vital cellular functions and metabolic processes. As a result, energy depletion occurs, hindering cellular growth and replication, and ultimately causing cell lysis and death. The strong interaction between piperazine and the membrane accounts for the polymer's broad-spectrum antimicrobial efficacy against various bacteria and fungi. Further detailed studies at the molecular level could provide deeper insights into the precise interactions and pathways involved in this antimicrobial activity.[35–37]

4.5. Surface morphology

Fig. 6 depicts the surface morphology of the coated substrate as investigated using scanning electron microscopy (SEM). The glass slide was chosen as the substrate for coating, and a 1.5 cm 1.5 cm glass piece was cut and sonicated in water, ethanol, and acetone for 15 minutes each. The PVC-*g*-AEP polymer sample solution was made by dissolving 10 mg of the sample in 1 mL of THF solvent and mixing it with commercially available paint (P) in an equimolar ratio. The prepared mixture (P + S) was coated on a glass slide and kept for drying at room temperature for 1 week. The results obtained from SEM analysis showed that the surface became porous in which polymeric particles were randomly scattered. If certain compounds, such as antibacterial agents like piperazine moiety are included in the polymer matrix, the porous structure might render it possible for them to be released in a controlled manner.

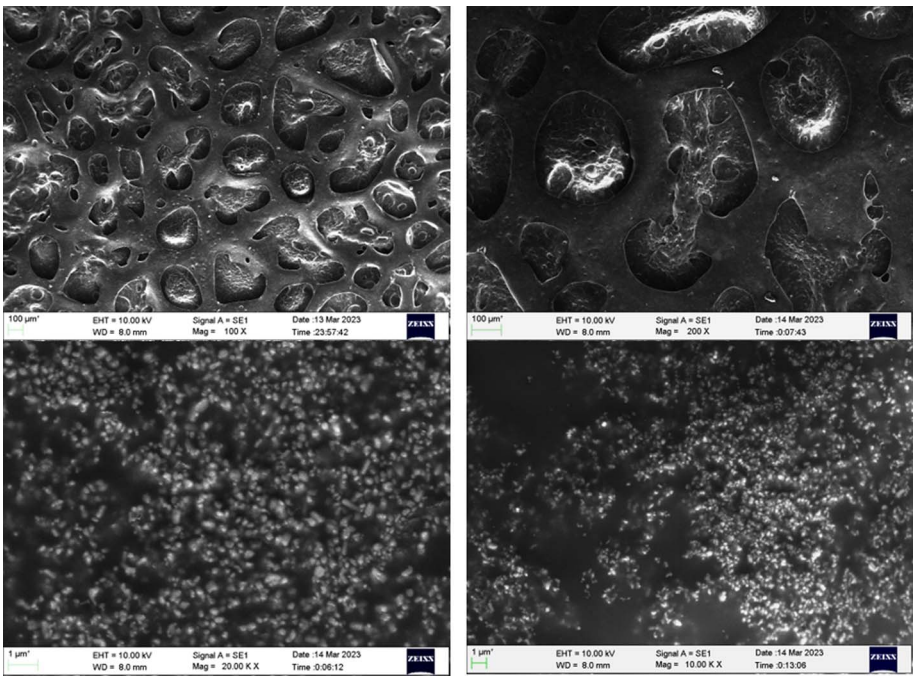

Fig. 6 SEM images of PVC-*g*-AEP polymer.

4.6. Surface roughness

An atomic force microscope (AFM) was utilized to ascertain the surface roughness of the coated glass slides, both with and without the presence of polymer. When analyzing the surface topology of a specific area, atomic force microscopy (AFM) was utilized. Additionally, Root Mean Square (RMS) analysis was performed to evaluate the surface roughness and measure variations in the surface's overall texture and topology. Both of these analyses were carried out with the assistance of Gwyddion software. To have a better knowledge of the consequent topographies that develop as a consequence of the porosity of the painted glass slides with and without polymer, this measurement is highly beneficial. There is an illustration of the porosity of the polymer sample with paint and paint in Fig. 7(a and b), respectively. The software determined that the surface roughness for paint without polymer was 1.4 nm, while with polymer, the surface roughness was 7.2 nm. The findings showed that the RMS surface roughness increased for paint with polymer samples. The addition of the antimicrobial polymer to the paint does not affect its visual and aesthetic properties, such as color, texture, and finish. Observations using SEM and AFM have shown that the primary change is an increase in the paint's porosity. This enhanced porosity can improve the antimicrobial efficacy without compromising the paint's appearance, ensuring that it remains visually appealing and marketable to consumers.

4.7. Antimicrobial activity of painted glass slide

The painted glass slide with and without polymer was tested for its antimicrobial activity against *C. albicans* (fungi), *E. coli* (Gram-negative bacteria), and *S. aureus* (Gram-positive bacteria). The efficacy of the painted slide with polymer was also determined, for that, the painted slide with polymer was washed 15 times in Milli-Q water and afterward tested for antimicrobial activity. To perform the activity, bacterial and fungal cultures were spread on agar plates and three different glass slides were taken and placed on microbial lawns. In Fig. 8, the glass slide P represents a painted glass slide without polymer, P + S represents a painted glass slide with polymer whereas washed P + S represents the glass slide which was washed 15 times in Milli-Q water, dried, and used for performing the activity.

The results obtained from the experiment show that P + S exhibited better activity in comparison to P, which means the synthesized polymer is more effective in preventing the growth of bacteria in comparison to commercially available paints. The washed P + S also showed prevention of bacteria and the highest activity was shown by *S. aureus* in comparison to other microbes. Therefore, PVC-*g*-AEP polymer holds Importance as a promising material in preventing the growth of bacteria for antimicrobial paint application.

The product demonstrated excellent antimicrobial activity, indicating strong potential for commercial applications. While initial raw material costs are notable, significant cost reductions can be achieved through bulk purchasing and sourcing from alternative suppliers. Effective planning, process optimization, and strategic sourcing can substantially lower overall production costs. The scalability of integrating antimicrobial polymers like PVC-*g*-AEP into existing paint production processes is promising, making large-scale implementation both feasible and economical. Using antimicrobial polymers such as PVC-*g*-AEP in commercial paint production presents numerous practical applications and scalability opportunities. In healthcare environments, these antimicrobial paints can be applied to walls and surfaces in hospitals and clinics to minimize

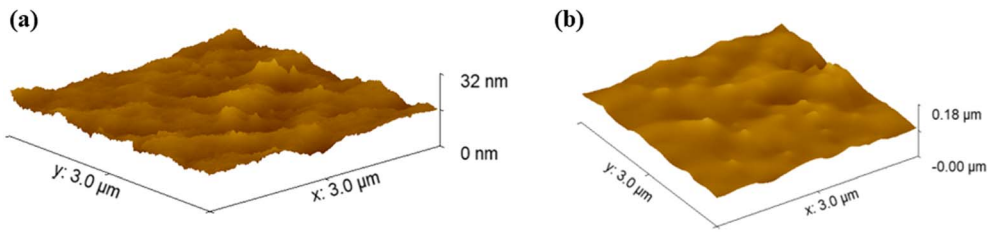

Fig. 7 AFM images of painted glass slide (a) with polymer and (b) without polymer.

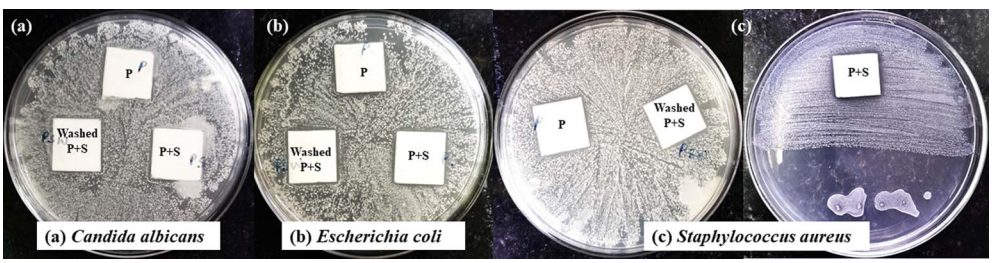

Fig. 8 The antimicrobial activity of painted glass slide with and without polymer. Three sets of glass slides were prepared; set 1 (P): painted glass slide without polymer; set 2 (P + S): painted glass slide with polymer and set 3 (washed P + S): painted glass slide with polymer and washed with water for 15 cycles, all these are tested for their antimicrobial activity against *C. albicans* (fungi), *E. coli* (Gram-negative bacteria), and *S. aureus* (Gram-positive bacteria).

infection risks by preventing the growth of harmful bacteria and microbes. This is crucial for maintaining sterile conditions in operating rooms and patient areas. In public settings, including schools, offices, and public transportation, antimicrobial paints can enhance hygiene and reduce the spread of pathogens, particularly in high-contact areas like handrails, doorknobs, and restrooms. For residential applications, these paints are beneficial in kitchens and bathrooms, where they can prevent mold and bacterial growth, promoting a healthier home environment. The scalability of using antimicrobial polymers in paint production is promising, as the base material, PVC, is already commonly used in the paint industry. By integrating antimicrobial agents into existing production processes with minimal modifications, large-scale implementation can be both practical and cost-effective.

5. Conclusion

In conclusion, this research underscores the significance of antimicrobial materials, particularly in the realm of paint technology, as a potent tool in safeguarding our surroundings against microbial threats. The synthesis of the poly(vinyl chloride) (PVC) grafted polymer containing 1-(2-aminoethyl piperazine) (AEP) has been meticulously explored through various analytical techniques, including FTIR, NMR, and thermal investigations, elucidating its structural attributes and thermal stability. The antimicrobial efficacy of the grafted polymer, when incorporated into commercial paint, has been comprehensively demonstrated against a spectrum of microbes. The surface morphology and roughness analyses further highlight the porous nature of the coated substrate, suggesting potential controlled release mechanisms. Notably, the painted glass slides exhibited sustained antimicrobial activity even after multiple washes, affirming the resilience and practicality of the PVC-*g*-AEP polymer as an antimicrobial paint. This research not only contributes to the evolving field of antimicrobial materials but also positions the synthesized polymer as a promising candidate for applications in enhancing the antimicrobial properties of paints, thereby promoting healthier and safer living environments.

Data availability

The data will be made available upon reasonable request from the corresponding author.

Conflicts of interest

The authors have nothing to declare.

References

1 B. Liu, C. Zhou, Z. Zhang, J. D. Roland and B. P. Lee, Antimicrobial property of halogenated catechols, *Chem. Eng. J.*, 2021, **403**, 126340, DOI: **10.1016/j.cej.2020.126340**.

2 D. Nathwani, G. Raman, K. Sulham, M. Gavaghan and V. Menon, Clinical and economic consequences of hospital-acquired resistant and multidrug-resistant Pseudomonas aeruginosa infections: a systematic review and meta-analysis, *Antimicrob. Resist. Infect. Control*, 2014, **3**(1), 32, DOI: **10.1186/2047-2994-3-32**.

3 R. Sugden, R. Kelly and S. Davies, Combatting antimicrobial resistance globally, *Nat. Microbiol.*, 2016, **1**(10), 16187, DOI: **10.1038/nmicrobiol.2016.187**.

4 K. Glinel, P. Thebault, V. Humblot, C. M. Pradier and T. Jouenne, Antibacterial surfaces developed from bio-inspired approaches, *Acta Biomater.*, 2012, **8**(5), 1670–1684, DOI: **10.1016/j.actbio.2012.01.011**.

5 H. Flemming, J. Wingender, U. Szewzyk, P. Steinberg, S. A. Rice and S. Kjelleberg, Biofilms: an emergent form of bacterial life, *Nat. Rev. Microbiol.*, 2016, **14**(9), 563–575, DOI: **10.1038/nrmicro.2016.94**.

6 M. Rosenberg, K. Ilić, K. Juganson, A. Ivask, M. Ahonen, I. Vinković Vrček, *et al.*, Potential ecotoxicological effects of antimicrobial surface coatings: a literature survey backed up by analysis of market reports, *PeerJ*, 2019, **7**, e6315. Available from: **https://peerj.com/articles/6315**.

7 E. K. Goharshadi, K. Goharshadi and M. Moghayedi, The use of nanotechnology in the fight against viruses: A critical review, *Coord. Chem. Rev.*, 2022, **464**, 214559, DOI: **10.1016/j.ccr.2022.214559**.

8 J. Zhao, W. Millians, S. Tang, T. Wu, L. Zhu and W. Ming, Self-Stratified Antimicrobial Acrylic Coatings via One-Step UV Curing, *ACS Appl. Mater. Interfaces*, 2015, **7**(33), 18467–18472, DOI: **10.1021/acsami.5b04633**.

9 P. Appendini and J. H. Hotchkiss, Review of antimicrobial food packaging, *Innovative Food Sci. Emerging Technol.*, 2002, **3**(2), 113–126. Available from: **https://linkinghub.elsevier.com/retrieve/pii/S1466856402000127**.

10 R. Kaur and S. Liu, Antibacterial surface design – Contact kill, *Prog. Surf. Sci.*, 2016, **91**(3), 136–153, DOI: **10.1016/j.progsurf.2016.09.001**.

11 D. Cunliffe, C. A. Smart, C. Alexander and E. N. Vulfson, Bacterial Adhesion at Synthetic Surfaces, *Appl. Environ. Microbiol.*, 1999, **65**(11), 4995–5002, DOI: **10.1128/AEM.65.11.4995-5002.1999**.

12 X. Chen, H. Hirt, Y. Li, S. Gorr and C. Aparicio, Antimicrobial GL13K Peptide Coatings Killed and Ruptured the Wall of Streptococcus gordonii and Prevented Formation and Growth of Biofilms, *PLoS One*, 2014, **9**(11), e111579, DOI: **10.1371/journal.pone.0111579**.

13 S. M. Dizaj, F. Lotfipour, M. Barzegar-Jalali, M. H. Zarrintan and K. Adibkia, Antimicrobial activity of the metals and metal oxide nanoparticles, *Mater. Sci. Eng., C*, 2014, **44**, 278–284. Available from: **https://linkinghub.elsevier.com/retrieve/pii/S0928493114005165**.

14 G. Grass, C. Rensing and M. Solioz, Metallic Copper as an Antimicrobial Surface, *Appl. Environ. Microbiol.*, 2011, **77**(5), 1541–1547, DOI: **10.1128/AEM.02766-10**.

15 M. P. Ajithkumar, M. P. Yashoda, S. Prasannakumar, T. V. Sruthi and V. B. Sameer Kumar, Synthesis, characterization, microstructure determination, thermal studies of poly (N-vinyl pyrrolidone-maleic anhydride-

methyl methacrylate), *J. Macromol. Sci., Part A*, 2018, **55**(4), 362–368, DOI: **10.1080/10601325.2018.1440178**.

16 A. Bouasria, A. Nadi, A. Boukhriss, H. Hannache, O. Cherkaoui and S. Gmouh, Advances in Polymer Coating for Functional Finishing of Textiles, in *Frontiers of Textile Materials*, Wiley, 2020, pp. 61–86, DOI: **10.1002/9781119620396.ch3**.

17 F. Hui and C. Debiemme-Chouvy, Antimicrobial N -Halamine Polymers and Coatings: A Review of Their Synthesis, Characterization, and Applications, *Biomacromolecules*, 2013, **14**(3), 585–601, DOI: **10.1021/bm301980q**.

18 Y. Wang, G. Jayan, D. Patwardhan and K. S. Phillips, Antimicrobial and Anti-Biofilm Medical Devices: Public Health and Regulatory Science Challenges, in *Antimicrobial Coatings and Modifications on Medical Devices*, Springer International Publishing, Cham, 2017, pp. 37–65, DOI: **10.1007/978-3-319-57494-3_2**.

19 M. Kazemzadeh-Narbat, H. Cheng, R. Chabok, M. M. Alvarez, C. de la Fuente-Nunez, K. S. Phillips, *et al.*, Strategies for antimicrobial peptide coatings on medical devices: a review and regulatory science perspective, *Crit. Rev. Biotechnol.*, 2021, **41**(1), 94–120, DOI: **10.1080/07388551.2020.1828810**.

20 N. A. Al-Tayyar, A. M. Youssef and R. Al-hindi, Antimicrobial food packaging based on sustainable Bio-based materials for reducing foodborne Pathogens: A review, *Food Chem.*, 2020, **310**, 125915, DOI: **10.1016/j.foodchem.2019.125915**.

21 M. Danková, A. Kalendová and J. Machotová, Waterborne coatings based on acrylic latex containing nanostructured ZnO as an active additive, *J. Coat. Technol. Res.*, 2020, **17**(2), 517–529, DOI: **10.1007/s11998-019-00302-6**.

22 F. Farsinia, E. K. Goharshadi, N. Ramezanian, M. M. Sangatash and M. Moghayedi, Antimicrobial waterborne acrylic paint by the additive of graphene nanosheets/silver nanocomposite, *Mater. Chem. Phys.*, 2023, **297**, 127355, DOI: **10.1016/j.matchemphys.2023.127355**.

23 C. C. Gaylarde, L. H. G. Morton, K. Loh and M. A. Shirakawa, Biodeterioration of external architectural paint films – A review, *Int. Biodeterior. Biodegrad.*, 2011, **65**(8), 1189–1198, DOI: **10.1016/j.ibiod.2011.09.005**.

24 A. C. F. Tornero, M. G. Blasco, M. C. Azqueta, C. F. Acevedo, C. S. Castro and S. J. R. López, Antimicrobial ecological waterborne paint based on novel hybrid nanoparticles of zinc oxide partially coated with silver, *Prog. Org. Coat.*, 2018, **121**, 130–141, DOI: **10.1016/j.porgcoat.2018.04.018**.

25 Y. Liu, J. C. Haley, K. Deng, W. Lau and M. A. Winnik, Effect of Polymer Composition on Polymer Diffusion in Poly(butyl acrylate- co -methyl methacrylate) Latex Films, *Macromolecules*, 2007, **40**(17), 6422–6431, DOI: **10.1021/ma070853c**.

26 L. Caballero, K. A. Whitehead, N. S. Allen and J. Verran, Photoinactivation of Escherichia coli on acrylic paint formulations using fluorescent light, *Dyes Pigm.*, 2010, **86**(1), 56–62, DOI: **10.1016/j.dyepig.2009.12.001**.

27 T. Eren, A. Som, J. R. Rennie, C. F. Nelson, Y. Urgina, K. Nüsslein, *et al.*, Antibacterial and Hemolytic Activities of Quaternary Pyridinium Functionalized Polynorbornenes, *Macromol. Chem. Phys.*, 2008, **209**(5), 516–524, DOI: **10.1002/macp.200700418**.

28 J. Liang, K. Barnes, A. Akdag, S. D. Worley, J. Lee and R. M. Broughton, Improved Antimicrobial Siloxane, *Appl. Chem.*, 2007, **46**(7), 1861–1866.

29 J. Hazziza-Laskar, G. Helary and G. Sauvet, Biocidal polymers active by contact. IV. Polyurethanes based on polysiloxanes with pendant primary alcohols and quaternary ammonium groups, *J. Appl. Polym. Sci.*, 1995, **58**(1), 77–84, DOI: **10.1002/app.1995.070580108**.

30 A. D. Fuchs and J. C. Tiller, Contact-Active Antimicrobial Coatings Derived from Aqueous Suspensions, *Angew. Chem., Int. Ed.*, 2006, **45**(40), 6759–6762, DOI: **10.1002/anie.200602738**.

31 K. Mukherjee, J. J. Rivera and A. M. Klibanov, Practical Aspects of Hydrophobic Polycationic Bactericidal "Paints.", *Appl. Biochem. Biotechnol.*, 2008, **151**(1), 61–70, DOI: **10.1007/s12010-008-8151-1**.

32 J. Hoque, P. Akkapeddi, V. Yadav, G. B. Manjunath, D. S. S. M. Uppu, M. M. Konai, *et al.*, Broad Spectrum Antibacterial and Antifungal Polymeric Paint Materials: Synthesis, Structure–Activity Relationship, and Membrane-Active Mode of Action, *ACS Appl. Mater. Interfaces*, 2015, **7**(3), 1804–1815, DOI: **10.1021/am507482y**.

33 M. Pandey, G. M. Joshi, A. Mukherjee and P. Thomas, Electrical properties and thermal degradation of poly(vinyl chloride)/polyvinylidene fluoride/ZnO polymer nanocomposites, *Polym. Int.*, 2016, **65**(9), 1098–1106, DOI: **10.1002/pi.5161**.

34 N. Peez and W. Imhof, Quantitative 1H-NMR spectroscopy as an efficient method for identification and quantification of PVC, ABS and PA microparticles, *Analyst*, 2020, **145**, 5363–5371.

35 M. S. Ibrahim, K. M. E. Salmawi and S. M. Ibrahim, Electron-beam modification of textile fabrics for hydrophilic finishing, *Appl. Surf. Sci.*, 2005, **241**(3–4), 309–320. Available from: **https://linkinghub.elsevier.com/retrieve/pii/S0169433204012498**.

36 S. Kanth, Y. M. Puttaiahgowda, T. Varadavenkatesan and S. Pandey, One-Pot Synthesis of Polyvinyl Alcohol-Piperazine Cross-Linked Polymer for Antibacterial Applications, *J. Polym. Environ.*, 2022, **30**(11), 4749–4762, DOI: **10.1007/s10924-022-02553-8**.

37 M. Zhang, G. Zeng, X. Liao and Y. Wang, An antibacterial and biocompatible piperazine polymer, *RSC Adv.*, 2019, **9**(18), 10135–10147. Available from: **http://xlink.rsc.org/?DOI=C9RA02219H**.